Advances in Computational Design, *Vol. 6, No. 3 (2021) 225-239*
https://doi.org/10.12989/acd.2021.6.3.

Computing the fracture energy of fiber reinforced cementitious composites using response surface methodology

Moosa Mazloom* and Sajjad Mirzamohammadi[a]

Department of Civil Engineering, Shahid Rajaee Teacher Training University, Tehran, Iran

(Received January 10, 2021, Revised May 30, 2021, Accepted June 8, 2021)

Abstract. In this study, some models are developed to predict the fracture energy (G_F), flexural strength (f_t), splitting tensile strength (f_{spt}), and compressive strength (f_c) of fiber reinforced cementitious composites (FRCC) based on I-optimal design of response surface methodology (RSM-I-optimal). Indeed, the main aim of this paper is to predict the mentioned parameters of FRCC at different temperatures and the aspect ratios of fibers. For this purpose, the fracture energy and strength properties of FRCC reinforced with aramid, glass, basalt, and polypropylene (PP) fibers were obtained at 20℃, 100℃ and 300℃ temperatures and were used as experimental values by RSM. The analyses of variance (ANOVA), perturbation, three-dimensional, contour and normal of residual plots were studied to assess the impacts of independent parameters on the relationships. Furthermore, the predictive efficiency of the RSM models between observed and predicted values were examined based on the Nash & Sutcliffe coefficient of efficiency (*NSE*). In terms of *NSE* values, the models were exact enough for predicting the flexural, splitting tensile and compressive strengths as well as fracture energy.

Keywords: fiber-reinforced cementitious composites; response surface methodology; I-optimal design; strength properties; fracture energy

1. Introduction

Concrete is a powerful generation of construction materials in structural engineering. Some significant features made this material to be used widely in the construction industry. These features include great compressive strength, fire resistance, and durability (Mazloom 2008, Mazloom and Ranjbar 2010, Mazloom *et al*. 2018a, Mazloom *et al*. 2018b). Although concrete, in general, is known for its advantages, it has some problems such as fragile fracture, cracking due to creep and shrinkage (Mazloom *et al*. 2004, Mazloom *et al*. 2019). Many researchers have tried to solve the mentioned difficulties. These issues encouraged the investigators to fabricate some new kinds of concrete including fiber reinforced concrete (FRC) and fiber-reinforced cementitious composite (FRCC) (Mazloom and Yoosefi 2013, Zhang *et al*. 2014, Mazloom and Mahboubi 2017,

*Corresponding author, Professor, E-mail: mazloom@sru.ac.ir, moospoon@yahoo.com
[a]M.Sc, E-mail: Sajadmirzamohamadi@gmail.com

http://www.techno-press.org/?journal=acd&subpage=7 ISSN: 2383-8477 (Print), 2466-0523 (Online)

Salehi and Mazloom 2018). The main ingredients of cementitious composites containing fibers (FRCC) are cementitious materials, water, fibers, and fine aggregate. In other words, the distinctive difference of FRCC in comparison with ordinary concrete or FRC is related to their aggregates. Note that adding fibers to the cementitious composite mixes can improve their low tensile strength (Yang *et al*. 2009, Yang and Li 2010, Li 2012, Mo *et al*. 2018, Zhang *et al*. 2019, Mazloom and Mirzamohammadi 2019, Mazloom and Mirzamohammadi 2020).

Response surface methodology (RSM) is a useful statistical and mathematical tool for investigating the relationship between the impacts of some separate factors on the the responses by changing these factors simultaneously. In other words, it studies the relationship between the factors (independent parameters) and the responses of the problems (Alsanusi and Bentaher 2015, Esat Alyamaç and Ghafari 2017, Mohammed *et al*. 2018, Şimşeka *et al*. 2018, Tyagi *et al*. 2018). I-optimal design (RSM-I-optimal) is one of the most common methods used under RSM for empirical modeling. Accordingly, the response model based on I-optimal is illustrated in Eq. (1) (Desai *et al*. 2008, Esfahanian *et al*. 2013, Awolusi *et al*. 2019, Mohammed *et al*. 2018).

$$Y= (b_0 + \varepsilon) + \sum_{i=1}^{k} b_i X_i + \sum_{i=1}^{k} b_{ii} X_i^2 + \sum_{i=1}^{k} \sum_{j=i+1}^{k} b_{ij} X_i X_j \quad (1)$$

where Y and k represent response values and number of independent parameters; b_0, b_i, b_{ii} and b_{ij} coefficients are determined by the least-squares method; X_i and X_j $(i \neq j)$ factors are independent parameters; ε is the error value.

In order to find appropriate equations, several studies have been conducted on different types of concrete by RSM. Alsanusi and Bentaher (2015) detected two relationships to estimate the compressive strength of ordinary concrete at the age of 28 days. The first model was in terms of mix components, while the second model was in terms of mix components and the concrete compressive strength at the age of 7 days. The values of coefficient of efficiency (E) were 0.85 and 0.91 for the first and second relationships, respectively. The variables were water, fine-aggregate, coarse-aggregate, cement, water to cement ratio and compressive strength at the age of 7 days. Jo *et al*. (2015) evaluated the flow and compressive strength of geopolymer concrete using central composite design (CCD) of RSM. Awolusi *et al*. (2019) discovered some relations to predict slump, water absorption, compressive strength, flexural strength and splitting tensile strength of concrete reinforced with steel fibers. The model classification was very good for slump, water absorption, compressive strength and splitting tensile strength, but it was acceptable for flexural strength. It should be noted that independent parameters were fiber aspect ratio, water to cement ratio and cement. Several studies have also been carried out using RSM procedure to optimize the mix proportions of concrete (Khayat *et al*. 2000, Mohammed *et al*. 2012, del Coz Diaz *et al*. 2014, Murray *et al*. 2014, Jimma and Rangaraju 2015, Al-alaily and Hassan 2016, Rezaifar *et al*. 2016).

Although many studies have been performed on examining the mechanical properties of FRCC, including changes in cementitious materials and fiber types in the mix designs (Li *et al*. 1996, Li 1998, Li 2000, Li *et al*. 2002, Li 2003, Maalej *et al*. 2005, Sahmaran and Li 2007, Li 2008, Şahmaran *et al*. 2010, Sahmaran *et al*. 2011, Yu *et al*. 2014, Yu *et al*. 2015), only a few studies have discovered some equations based on RSM (the I-optimal) to predict their mechanical properties. In other words, most of the studies in RSM field are related to predicting the compressive strength of ordinary concrete (Bayramov *et al*. 2004, Mandal and Roy 2006, Nambiar and Ramamurthy 2006, Aldahdooh *et al*. 2013, Cihan *et al*. 2013, Rostamian *et al*. 2015, Nassar *et al*. 2016). Accordingly, this study investigates some equations to predict fracture energy (G_F), flexural strength (f_t), splitting tensile strength (f_{spt}), and compressive strength (f_c) of FRCC at the age of 28 days based on the RSM-I-optimal.

Table 1 Mix proportions for FRCC

Mix ID	Kg/m^3						2%vol
	Cement	Silica fume	Silica sand	Water	HRWRA	W/(C+SF)	Fiber
A-FRCC	850	160	588	390	16	0.38	Aramid
G-FRCC	850	160	588	390	16	0.38	Glass
B-FRCC	850	160	588	390	16	0.38	Basalt
P-FRCC	850	160	588	390	16	0.38	PP

Table 2 Chemical composition of cement and SF

	OPC	SF
Silicon dioxide (SiO_2): wt%	21.30	96.4
Calcium oxide (CaO): wt%	63.48	0.49
Aluminium oxide (Al_2O_3): wt%	5.13	1.32
Ferric oxide (Fe_2O_3): wt%	3.47	0.87
Sodium oxide (Na_2O): wt%	0.23	0.31
Mangnesium oxide (MgO): wt%	2.51	0.97
Phosphorus pentoxide (P_2O_5): wt%	-	0.16
Sulfur trioxide (SO_3): wt%	1.67	0.10
Potassium oxide (K_2O): wt%	0.56	1.01
Silicon carbide (SiC): wt%	-	0.5
Carbon (C): wt%	-	0.3
Chloride (CL): wt%	-	0.04
Water (H_2O): wt%	-	0.08

Table 3 Properties of fibers

Fiber type	Diameter, µm	Length, mm	Tensile Strength, MPa	Young Modulus, GPa	Density, Kg/m^3	Melting Point, ℃	Aspect ratio* (L_f/D_f)
Aramid	12	10	3150	80	1440	800	833
Basalt	11	10	2950	90	2670	600	909
Glass	20	10	3450	69	2550	1400	500
PP	23	10	400	2.7	910	165	434

*Aspect ratio of fiber is defined as its length divided by its diameter

2. Experimental program

2.1 Material

The FRCC mix proportions are presented in Table 1. Silica fume (SF) and Ordinary Portland cement (OPC) were used as cementitious materials. Silica fume can develop the quality of hydration products (Mazlom *et al*. 2015, Mazloom and Miri 2017, Mazloom *et al*. 2017, Afzali

Table 4 Independent parameters with code levels

Independent variables	Symbols	Code levels		
		-1	0	+1
A = Temperature (°C)	A	20	160	300
B = Fiber aspect ratio (μm/mm)	B	400	650	900

Table 5 Details of experimental values in coded

Num	Mix ID	Factors		Responses			
		A	B	Compressive strength (MPa)	Splitting tensile strength (MPa)	Flexural Strength (MPa)	Fracture energy (MPa)
1	A-FRCC	20	800	65	8	9	4.21
2	A-FRCC	20	800	71	9	10	4.31
3	A-FRCC	20	800	69	8	9	4.2
4	G-FRCC	20	500	56	6.5	9	6.3
5	G-FRCC	20	500	59.5	7	10	6.5
6	G-FRCC	20	500	60.5	7	10	6.64
7	B-FRCC	20	900	53	6	7.5	5.1
8	B-FRCC	20	900	54.5	7	8	5.4
9	B-FRCC	20	900	49.5	6	8	5.37
10	P-FRCC	20	400	58	6	8	7.6
11	P-FRCC	20	400	53	5.5	7.5	7.4
12	P-FRCC	20	400	60	7	8.5	7.71
13	A-FRCC	100	800	71	7	7	2.8
14	A-FRCC	100	800	70	7	7.5	3.01
15	A-FRCC	100	800	75	8	8.5	3.1
16	G-FRCC	100	500	64.5	6	9.5	6.1
17	G-FRCC	100	500	61	5.5	6.5	5.7
18	G-FRCC	100	500	61	5	8	5.96
19	B-FRCC	100	900	49.5	6	7	2.64
20	B-FRCC	100	900	48	5.5	6	2.5
21	B-FRCC	100	900	48	6	6	2.45
22	P-FRCC	100	400	60	5	5	3.99
23	P-FRCC	100	400	66	6	6	3.95
24	P-FRCC	100	400	63	5	5.5	3.85
25	A-FRCC	300	800	71.5	4.5	5	1.7
26	A-FRCC	300	800	73	5	6	1.85
27	A-FRCC	300	800	72.5	4.5	6	1.97
28	G-FRCC	300	500	55	4.5	5	2.2
29	G-FRCC	300	500	56	4.5	4	2.09
30	G-FRCC	300	500	57	5	5	2.01
31	B-FRCC	300	900	43	3	4	1.25
32	B-FRCC	300	900	50	4	4.5	1.6
33	B-FRCC	300	900	47	3	4	1.5
34	P-FRCC	300	400	62.5	5	5	2.3
35	P-FRCC	300	400	63	5	5	2.2
36	P-FRCC	300	400	70	5.5	5.5	2.49

Naniz and Mazloom 2018, Afzali Naniz and Mazloom 2019a). Table 2 presents the chemical compositions of the mentioned materials. Furthermore, silica sand and polycarboxylate-based high-range water reducing admixture (HRWRA) were used as fine aggregate and superplasticizer, respectively. The fibers used in the mix designs were aramid, basalt, glass, and polypropylene (PP) fibers. The mechanical and geometrical properties of these fibers are presented in Table 3. To determine the experimental (observed) values including compressive strength, rupture modulus, splitting tensile strength, and fracture energy of cement composites containing fibers (FRCC) at 20°C, 100°C, and 300°C temperatures, the samples were cast and wet cured for 28 days. Next, the specimens (except for the temperature of 20°C) were maintained in an electric oven for 1 h at 100°C and 300°C. Then, the specimens were ready for the tests.

2.2 Methodology

The I-optimal design was selected to discover the relationship between two independent parameters and responses. The independent parameters with code levels are shown in Table 4. The responses include fracture energy (G_F), flexural strength or rupture modulus (f_t), splitting tensile (f_{spt}) and compressive (f_c) strengths. All of the 36 experimental values used by RSM, in 14 experimental runs, are presented in Table 5. In order to determine the predictive efficiency of the RSM model between experimental (observed) and predicted values, Nash & Sutcliffe coefficient of efficiency (NSE) was used, as defined in Eqs. (2) to (5) (Ritter and Muñoz -Carpena 2013).

$$NSE = 1- \left(\frac{RMSE}{SD}\right)^2 \tag{2}$$

$$RMSE = (MSE)^{\frac{1}{2}} \tag{3}$$

$$MSE = \frac{\sum_{i=1}^{n}(Y_i - O_i)^2}{n} \tag{4}$$

$$SD = \left(\frac{\sum_{i=1}^{n}(O_i - \bar{O})^2}{n}\right)^{\frac{1}{2}} \tag{5}$$

where MSE, $RMSE$ and SD are mean square error, root-mean-square error and standard deviation, respectively. Moreover, $Y_i, O_i, \bar{O}$ and n are predicted, experimental, mean of the experimental and number of values, respectively. In terms of NSE, the model performance rating is classified unsatisfactory, acceptable, good and very good when $NSE < 0.65$, $0.65 \leq NSE < 0.8$, $0.8 \leq NSE < 0.9$ and $NSE \geq 0.9$, respectively.

3. Results and discussion

3.1 Fracture energy

In recent years, several studies have examined the fracture behavior of ordinary, lightweight, and self-compacting normal concrete (Nikbin *et al*. 2016, Karamloo *et al*. 2016, Karamloo *et al*. 2017, Karamloo and Mazloom 2018, Mazloom and Karamloo 2019, Salehi and Mazloom 2019a, Salehi and Mazloom 2019b, Afzali Naniz and Mazloom 2019b). However, sparse studies have investigated the fracture energy of FRCC (Bolander *et al*. 2008). In this research, to calculate the

Table 6 ANOVA for fracture energy

Source	Sum of Squares	Degree of freedom	Mean Square	F-value	p-value	
Model	160.08	5	32.02	705.45	< 0.0001	significant
A-Temperature	104.87	1	104.87	2310.82	< 0.0001	
B-Fiber aspect ratio	22.50	1	22.50	495.72	< 0.0001	
AB	5.94	1	5.94	130.94	< 0.0001	
A^2	6.27	1	6.27	138.16	< 0.0001	
B^2	0.6862	1	0.6862	15.12	0.0004	
Residual	1.63	36	0.0454			
Lack of Fit	0.1357	6	0.0226	0.4528	0.8372	not significant
Pure Error	1.50	30	0.0499			
Cor Total	161.71	41				

fracture energies of the specimens, ASTM C1609 (2006) is used. In this regard, the fracture energy can be determined as given in Eqs. (6) to (8) (Hillerborg 1985).

$$G_F = \frac{W}{a} \tag{6}$$

$$W = W_0 + W_1 + W_2 \tag{7}$$

$$W_1 = W_2 = F_1\delta_0 \tag{8}$$

Where G_F, W and a are fracture energy, total area under the load-deflection curve and broken cross-section. Furthermore, the deformation when the beam breaks is δ_0, the initial area under the load-deflection curve is W_0, and F_1 is the weight of testing equipment and the beam (Mazloom and Mirzamohammadi 2020).

Eq. (9) represents a formula for predicting the fracture energy of FRCC based on RSM-I-optimal. In this equation, A and B are temperature (°C) and fiber aspect ratio (μm/mm), respectively. The coefficient of determination (R^2) for this equation was 0.98. Table 6 presents the analysis of variance (ANOVA) for the fracture energy. According to this table, both temperature and fiber aspect ratio have significant impacts on the fracture energy (p-value<0.05). Moreover, the effect of temperature is far greater than fiber aspect ratio. High temperatures have negative influence on the fracture energy of all specimens. The perturbation plot for fracture energy is illustrated in Fig. 1. The findings mentioned above can be seen in this figure.

$$\text{Fracture energy} = +8.2198 - 0.0414017A + 0.00214909B + 1.60201 \times 10^{-5}AB + 5.20594 \times 10^{-5}A^2 - 6.49742 \times 10^{-6}B^2 \tag{9}$$

3.2 Flexural strength

To evaluate the flexural strengths of the specimens, ASTM C1609 (ASTM C1609/M-05 2006) was used. Eq. (10) indicates a relationship for the flexural strength of FRCC. The coefficient of determination (R^2) for this equation was calculated to be 0.92. Fig. 2 depicts three-dimensional

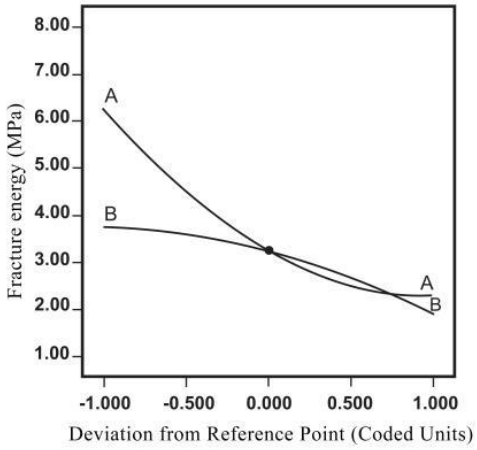

Fig. 1 Perturbation plot for fracture energy

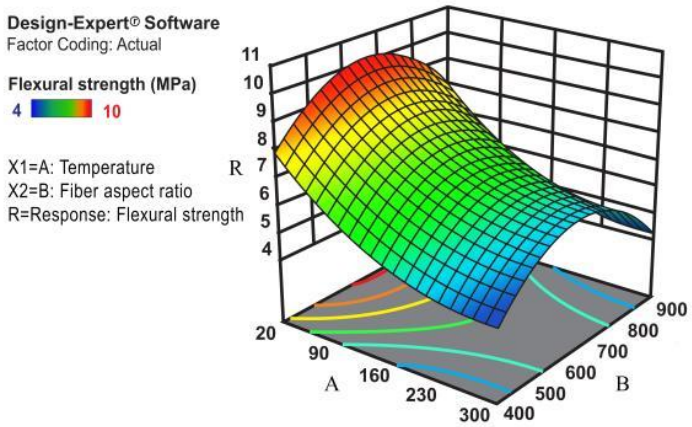

Fig. 2 3D plot of flexural strength in I-optimal design

plot (3D) for flexural strength in the I-optimal design. As can be seen in this figure, the highest and lowest flexural strengths of the samples were related to temperatures of 20°C and 300°C, respectively.

$$\text{Flexural strength} = -3.9714 - 0.0296095A + 0.0451316B + 5.10413 \times 10^{-5}A^2 - 3.46596 \times 10^{-5}B^2 \quad (10)$$

3.3 Splitting tensile strength

To assess the tensile strength of the samples, BS 1881: part 117: 1983 (BS 1983a) was used. Eq. (11) indicates a relationship for the splitting tensile strength of FRCC. The coefficient of determination (R^2) for this equation was 0.83. Fig. 3 displays the contour plot for splitting tensile strength in the RSM. This figure reveals that splitting tensile strengths of the specimens decreased when the temperature increased. Mechtcherine *et al*. (2012) investigated the effects of temperature on the tensile behavior of

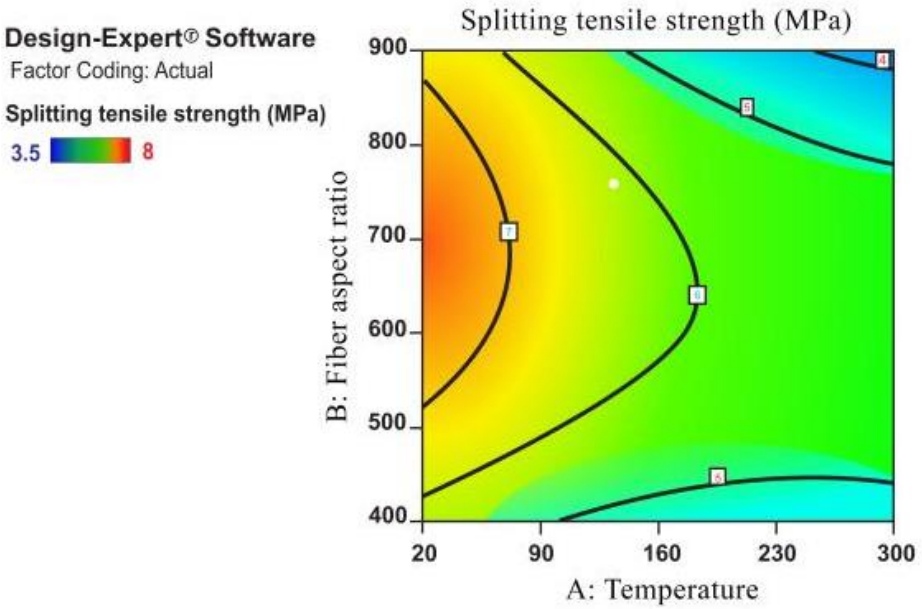

Fig. 3 Contour plot for splitting tensile strength

strain-hardening cement-based composites (SHCC) reinforced with PVA fibers. They similarly detected the tensile strength of the samples dropped at 100 and 150°C.

$$\text{Splitting tensile strength} = -3.34234 - 0.00565433A + 0.0322036B - 1.42734 \times 10^{-5}AB + 2.43318 \times 10^{-5}A^2 - 2.28726 \times 10^{-5}B^2 \quad (11)$$

3.4 Compressive strength

The experimental values for the compressive strength of the specimens are shown in Table 5. The dimensions of the cube samples used for this test were 15×15×15 cm^3 according to BS 1881: part 108: 1983 (BS 1983b). Eq. (12) presents a relationship to predict compressive strength of FRCC based on the RSM method. In this equation, the coefficient of determination (R^2) is 0.98. Table 7 shows the analysis of variance (ANOVA) for compressive strength. As can be seen in this table, the effects of fiber aspect ratio on the compressive strength are far greater than temperature, and fiber aspect ratio has a higher F-value than temperature. In other words, sub-elevated temperatures did not have considerable impacts on the compressive strength of the specimens. Some studies are in agreement with the mentioned results. For instance, Morsy *et al*. (2012) detected that the compressive strengths of the blended and control cement mortars were enhanced with temperatures up to 250°C and then declined as the temperature rose up to 800°C. Fig. 4 depicts the normal plot of residuals for the compressive strength. The normal probability plot is a graphical technique for assessing whether or not a data set is approximatly normally distributed. The data are plotted against a theoretical normal distribution in such a way that the points should form an approximate straight line. Departures from this straight line indicate departures from normality. As can be seen in this figure, all plotted points fell very close to the distribution fitted line.

Table 7 ANOVA for compressive strength

Source	Sum of Squares	Degree of freedom	Mean Square	F-value	p-value	
Model	864.43	5	172.89	372.31	< 0.0001	significant
A-Temperature	9.50	1	9.50	20.46	< 0.0001	
B-Fiber aspect ratio	278.69	1	278.69	600.16	< 0.0001	
AB	103.37	1	103.37	222.62	< 0.0001	
A^2	0.0102	1	0.0102	0.0219	0.8832	
B^2	517.42	1	517.42	1114.27	< 0.0001	
Residual	16.72	36	0.4644			
Lack of Fit	3.88	6	0.6472	1.51	0.2078	not significant
Pure Error	12.83	30	0.4278			
Cor Total	881.14	41				

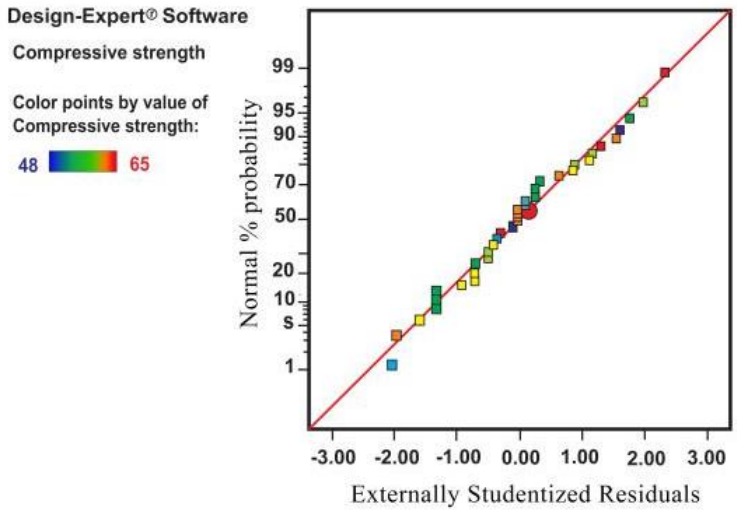

Fig. 4 Normal plot of residuals for the compressive strength

$$\text{Compressive strength} = -7.62398 + 0.0391253A + 0.229317B - 6.6784 \times 10^{-5}AB - 0.000178288 \times B^2 \quad (12)$$

3.5 Predictive efficiency of the RSM model

This study presents the predictive efficiency of the RSM model between the observed and predicted values based on *NSE* method (Ritter and Carpena, 2013). Standard deviation (*SD*), mean square error (*MSE*), root-mean-square error (*RMSE*), Nash & Sutcliffe coefficient of efficiency (*NSE*), and model classification are reported in Table 8. According to this table, the model classifications are very good, good, good, and acceptable for fracture energy (FE), flexural (FS), splitting tensile (STS) and compressive strengths (CS), respectively.

Table 8 Predictive efficiency of the RSM model

Test	*SD*	*MSE*	*RMSE*	*NSE*	Model classification
FE	2.06	0.42	0.65	0.90	Very good
FS	2.15	0.51	0.71	0.89	Good
STS	1.65	0.47	0.68	0.82	Good
CS	13.1	53.3	7.30	0.69	Acceptable

5. Conclusions

From the results of this study, the following conclusions can be derived:

• The analysis of variance (ANOVA) for fracture energy indicated that both temperature and fiber aspect ratio had significant impacts on the fracture energy. However, the impact of temperature was greater than fiber aspect ratio. In other words, sub-elevated temperatures had considerable negative effects on the fracture energy of the specimens.

• Regarding the fracture energy, the results of the RSM models showed that the use of polypropylene fibers in fiber reinforced cementitious composites (FRCC) was more efficient than utilizing glass, aramid, and basalt fibers at both normal and sub-elevated temperatures.

• Three-dimensional (3D) and contour plots for flexural and splitting tensile strengths showed the considerable negative influences of sub-elevated temperatures on the mentioned strengths. Perhaps the reason for this phenomenon is that high temperatures can reduce the van der Waal's forces between C-S-H layers; therefore, the mentioned strengths can diminish. The samples reinforced with glass and aramid fibers had the greatest flexural and splitting tensile strengths at both normal and sub-elevated temperatures.

• The analysis of variance (ANOVA) for compressive strength indicated that the influence of fiber aspect ratio on the compressive strength was greater than temperature. In other words, sub-elevated temperatures did not have considerable negative impact on the compressive strength of the specimens. The reason for this can be the hydration of cement particles that did not contribute to the hydration process before reaching to 100 ℃ and 300 ℃ temperatures.

• In almost all cases, the specimens reinforced with polypropylene fibers showed the best performances against elevated temperatures. In other words, the minimum reductions in fracture energy, flexural, splitting tensile, and compressive strengths were related to the samples containing polypropylene fibers at both 100℃ and 300℃ temperatures.

• The predictive efficiencies of the RSM models were very good, good, good, and acceptable for fracture energy, flexural, splitting tensile and compressive strengths, respectively.

References

Afzali-Naniz, O. and Mazloom, M. (2018), "Effects of colloidal nano-silica on fresh and hardened properties of self-compacting lightweight concrete", *J. Build. Eng.*, **20**, 400-410. https://doi.org/10.1016/j.jobe.2018.08.014.

Afzali-Naniz, O. and Mazloom, M. (2019a), "Assessment of the influence of micro- and nano-silica on the behavior of self-compacting lightweight concrete using full factorial design", *Asian J. Civ. Eng.*, **20**, 57-70. https://doi.org/10.1007/s42107-018-0088-2.

Afzali-Naniz, O. and Mazloom, M. (2019b), "Fracture behavior of self-compacting semi-lightweight

concrete containing nano-silica", *Adv. Struct. Eng.*, 22(10), 2264-2277. https://doi: 10.1177/1369433219837426.

Al-alaily, H.S. and Hassan, A.A. (2016), "Refined statistical modeling for chloride permeability and strength of concrete containing metakaolin", *Construct. Build. Mater.*, **114**, 564-579. https://doi.org/10.1016/j.conbuildmat.2016.03.187.

Aldahdooh, M., Bunnori, M.N. and Megat M.J. (2013), "Evaluation of ultrahigh- performance-fiber reinforced concrete binder content using the response surface method", *Mater. Des.*, **52**, 957-965. https://doi.org/10.1016/j.matdes.2013.06.034.

Alsanusi, S. and Bentaher, L. (2015), "Prediction of compressive strength of concrete from early age test result using design of experiments (RSM)", *Int. J. Civ. Environ. Struct. Constr. Archit. Eng.*, **9**(12), 1559-1563.

ASTM C1609/M-05 (2006), *Standard Test Method for Flexural Performance of Fiber Reinforced Concrete (using Beam with Third-point loading)*, ASTM International, West Conshohocken Pennsylvania.

Awolusi, T.F., Oke, O.L., Akinkurolere, O.O. and Sojobi, A.O. (2019), "Application of response surface methodology: Predicting and optimizing the properties of concrete containing steel fiber extracted from waste tires with limestone powder as filler", *Case Stud. Constr. Mater.*, **10**. https://doi.org/10.1016/j.cscm.2018.e00212.

Balaji, A., Luquman K, M., Nagarajan, P. and Madhavan Pillai, T.M. (2016), "Prediction of response of reinforced concrete frames exposed to fire", *Advan. Comput. Des.*, **1**(1), 105-117. http://dx.doi.org/10.12989/acd.2016.1.1.105.

Bayramov, F., Tasdemir, C. and Tasdemir, M.A. (2004), "Optimization of steel fibre reinforced concretes by means of statistical response surface method", *Cem. Concrete. Compos.*, **26**(6), 665-675. https://doi.org/10.1016/S0958-9465(03)00161-6.

Bolander, J.E., Choi, S. and Duddukuri, S.R. (2008), "Fracture of fiber-reinforced cement composites: effects of fiber dispersion", *Int. J. Fract.*, **154**, 73-86. https://doi.org/10.1007/s10704-008-9269-4.

BS 1881: part 108. (1983b), *Method for Making Test Cubes from Fresh Concrete*, British Standards.

BS 1881: part 117. (1983a), *Method for Determination of Tensile Splitting Strength*, British Standards.

Cihan, M.T., Güner, A. and Yüzer N. (2013), "Response surfaces for compressive strength of concrete", *Construct. Build. Mater.*, **40**, 763-774. https://doi.org/10.1016/j.conbuildmat.2012.11.048.

Del Coz Diaz, J.J., Garcia-Nieto, P.J., Alvarez-Rabanal, F.P., Alonso-Martínez, M., Dominguez Hernandez, J. and Perez-Bella, J.M. (2014), "The use of response surface methodology to improve the thermal transmittance of lightweight concrete hollow bricks by FEM", *Construct. Build. Mater.*, **52**, 331-344. https://doi.org/10.1016/j.conbuildmat.2013.11.056.

Desai, K.M., Survase, S.A., Saudagar, P.S., Lele, S.S. and Singhal, R.S. (2008), "Comparison of artificial neural network ANN and response surface methodology in fermentation media optimization: Case study of fermentative production of scleroglucan", *Biochem. Eng. J.*, **41**(3), 266-273. https://doi.org/10.1016/j.bej.2008.05.009.

Esat Alyamaç, K. and Ghafari, E. (2017), "Development of eco-efficient self-compacting concrete with waste marble powder using the response surface method", *J. Cleaner Prod.*, **144**, 192-202. https://doi.org/10.1016/j.jclepro.2016.12.156.

Esfahanian, M., Nikzad, M., Najafpour, G. and Ghoreyshi, A. (2013), "Modeling and optimization of ethanol fermentation using Saccharomyces cerevisiae: Response surface methodology and artificial neural network", *Chem. Ind. Chem. Eng. Q.*, **19**, 241-252. https://doi.org/10.2298/CICEQ120210058E.

Hillerborg, A. (1985), "The theoretical basis of a method to determine the fracture energy GF of concrete", *Mater. Struct.*, **18**(4), 291-296.

Jimma, B.E. and Rangaraju, P.R. (2015), "Chemical admixtures dose optimization in pervious concrete paste selection-A statistical approach", *Constr. Build. Mater.*, **101**, 1047-1058. https://doi.org/10.1016/j.conbuildmat.2015.10.003.

Jo, M., Soto, L., Arocho, M., St John, J. and Hwang, S. (2015), "Optimum mix design of fly ash geopolymer paste and its use in pervious concrete for removal of fecal coliforms and phosphorus in water", *Construct. Build. Mater.*, **93**, 1097-1104. https://doi.org/10.1016/j.conbuildmat.2015.05.034.

Karamloo, M. and Mazloom, M. (2018), "An efficient algorithm for scaling problem of notched beam specimens with various notch to depth ratios", *Comput. Concr.*, **22**(1), 39-51. http://dx.doi.org/10.12989/cac.2018.22.1.039.

Karamloo, M., Mazloom, M. and Payganeh, G. (2016), "Effects of maximum aggregate size on fracture behaviors of self-compacting lightweight concrete", *Constr. Build. Mater.*, **123**, 508-515. https://doi.org/10.1016/j.conbuildmat.2016.07.061.

Karamloo, M., Mazloom, M. and Payganeh, G. (2017), "Effect of size on nominal strength of self-compacting lightweight concrete and self-compacting normal weight concrete: A stress-based approach", *Mater. Today Commun.*, **13**, 36-45. https://doi.org/10.1016/j.mtcomm.2017.08.002.

Kaveh, A. and Bakhshpoori, T. (2016), "An efficient multi-objective cuckoo search algorithm for design optimization", *Advan. Comput. Des.*, **1**(1), 87-103. http://dx.doi.org/10.12989/acd.2016.1.1.087.

Kaveh, A. and Rezaei, M. (2016), "Topology and geometry optimization of different types of domes using ECBO", *Advan. Comput. Des.*, **1**(1), 1-25. http://dx.doi.org/10.12989/acd.2016.1.1.001.

Khayat, K., Ghezal, A. and Hadriche, M. (2000), "Utility of statistical models in proportioning self-consolidating concrete", *Mater. Struct.*, **33**(5), 338-344. https://doi.org/10.1007/BF02479705.

Li, V.C. (1998), "Engineered Cementitious Composites - Tailored Composites Through Micromechanical Modeling Fiber Reinforced Concrete: Present and the Future edited by Banthia, N. in Fiber Reinforced Concrete", *Canadian Soc. Civil Eng.*, 64-97. http://hdl.handle.net/2027.42/84667.

Li, V.C. (2000), "Strategies for high performance fiber reinforced cementitious composites development", *Proceedings of International Workshop on Advances in Fiber Reinforced Concrete*, Bergamo, Italy, 93-98. http://hdl.handle.net/2027.42/84792.

Li, V.C. (2003), "On engineered cementitious composites (ECC) -a review of the material and its applications", *Advan. Concrete*, **1**(3), 215-230.

Li, V.C. (2008), "Durability of mechanically loaded engineered cementitious composites under highly alkaline environments", *Cement Concrete. Compos.*, **30**, 72-81. https://doi.org/10.1016/j.cemconcomp.2007.09.004.

Li, V.C. (2012), "Tailoring ECC for Special Attributes", *Int. J. Concrete Struct. Mater.*, **6**, 135-144. https://doi.org/10.1007/s40069-012-0018-8.

Li, V.C., Wu, C., Wang, S. and Ogawa, A. (2002), "Interface tailoring for strain-hardening polyvinyl alcohol-engineered cementitious composites (PVA-ECC)", *ACI Mater.*, **99**(5), 463-472. http://hdl.handle.net/2027.42/84693.

Li, V.C., Wu, H.C., Maalej, M.D. and Mishra, D. (1996), "Tensile behavior of cement-based composite with random discontinuous steel fibers", *J. Amer. Ceram. Soc.*, **79**, 74-78. https://doi.org/10.1111/j.1151-2916.1996.tb07882.x.

Maalej, M., Quek, S.T. and Zhang, J. (2005), "Behavior of hybrid-fiber engineered cementitious composites subjected to dynamic tensile loading and projectile impact", *J. Mater. Civ. Eng.*, **17**, 143-152.

Mandal, A. and Roy, P. (2006), "Modeling the compressive strength of molasses-cement sand system using design of experiments and back propagation neural network", *J. Mater. Process. Technol.*, **180**,167-173. https://doi.org/10.1016/j.jmatprotec.2006.05.017.

Mazloom, M. (2008), "Estimating long-term creep and shrinkage of high-strength concrete", *Cement Concrete Compos.*, **30**(4), 316-326. https://doi.org/10.1016/j.cemconcomp.2007.09.006.

Mazloom, M. and Karamloo, M. (2019), "Critical crack-tip opening displacement of SCLC", *Malaysia*, 135-143. https://doi.org/10.1007/978-981-10-8016-6_11.

Mazloom, M. and Mahboubi, F. (2017), "Evaluating the settlement of lightweight coarse aggregate in self-compacting lightweight concrete", *Comput, Concrete*, **19**(2), 203-210. https://doi.org/10.12989/cac.2017.19.2.203.

Mazloom, M. and Miri, M.S. (2017), "Interaction of magnetic water, silica fume and superplasticizer on fresh and hardened properties of concrete", *Advan. Concrete. Construct*, **5**(2), 87-99. https://doi.org/10.12989/acc.2017.5.2.087.

Mazloom, M. and Mirzamohammadi, S. (2019), "Thermal effects on the mechanical properties of cement

mortars reinforced with aramid, glass, basalt and polypropylene fibers", *Advan. Mater. Res.*, **8**(2), 137-154. http://dx.doi.org/10.12989/amr.2019.8.2.137.

Mazloom, M. and Mirzamohammadi, S. (2020), "Fracture of fibre-reinforced cementitious composites after exposure to elevated temperatures", *Mag. Concrete Res.*, https://doi.org/10.1680/jmacr.19.00401.

Mazloom, M. and Ranjbar, A. (2010), "Relation between the workability and strength of self-compacting concrete", *The 35th Conference on our World in Concrete & Structures.*, Singapore, 315-322.

Mazloom, M. and Yoosefi, M.M. (2013), "Predicting the indirect tensile strength of self compacting concrete using artificial neural networks", *Comput. Concrete*, **12**(3), 285-301. https://doi.org/10.12989/cac.2013.12.3.285.

Mazloom, M., Allahabadi, A. and Karamloo, M. (2017), "Effect of silica fume and polyepoxide-based polymer on electrical resistivity", *Advan. Concrete Construct.*, **5**(6), 587-611. https://doi.org/10.12989/acc.2017.5.6.587.

Mazloom, M., Homayooni, S.M. and Miri, S.M. (2018a), "Effect of rock flour type on rheology and strength of self-compacting lightweight concrete", *Comput. Concrete*, **21**(2), 199-207. https://doi.org/10.12989/cac.2018.21.2.199.

Mazloom, M., Pourhaji, P., Shahveisi, M., and Jafari, S.H. (2019), "Studying the Park-Ang damage index of reinforced concrete structures based on equivalent sinusoidal waves", *Struct. Eng. Mech.*, **72**(1), 845-859. http://doi: 10.12989/sem.2019.72.1.083.

Mazloom, M., Ramezanianpour, A.A. and Brooks J.J. (2004), "Effect of silica fume on mechanical properties of high-strength concrete". *Cement Concrete Compos.*, **26**(1), 347-357. https://doi.org/10.1016/S0958-9465(03)00017-9.

Mazloom, M., Saffari, A. and Mehrvand, M. (2015), "Compressive, shear and torsional strength of beams made of self-compacting concrete", *Comput. Concrete*, **15**(6), 935-950. https://doi.org/10.12989/cac.2015.15.6.935.

Mazloom, M., Soltani, A., Karamloo, M., Hasanloo, A. and Ranjbar, A. (2018b), "Effects of silica fume, superplasticizer dosage and type of superplasticizer on the properties of normal and self-compacting concrete", *Advan. Mater. Res.*, **7**(1), 407-434. https://doi.org/10.12989/amr.2018.7.1.045.

Mechtcherine, V., Andrade, F.De., Müller, S.P., Jun, P., Dias, R. and Filho, T. (2012), "Coupled strain rate and temperature effects on the tensile behavior of strain-hardening cement-based composites (SHCC) with PVA fibers", *Cement Concrete Res.*, **42**, 1417-1427. https://doi.org/10.1016/j.cemconres.2012.08.011.

Mo, K.H., Loh, Z.P. and Tan, C.G., Alengaram, U.J. and Yap, S.P. (2018), "Behavior of fiber-reinforced cementitious composite containing high-volume fly ash at elevated temperatures", Sadha., **43**(11). https://doi.org/ 10.1007/s12046-018-0937-4.

Mohammed, B.S., Fang, O.C., Hossain, K.M.A and Lachemi, M. (2012), "Mix proportioning of concrete containing paper mill residuals using response surface methodology", *Construct. Build. Mater.*, **35**, 63-68. https://doi.org/10.1016/j.conbuildmat.2012.02.050.

Mohammed, B.S., Khed, V.C. and FadhilNuruddin, M. (2018), "Rubbercrete mixture optimization using response surface methodology", *J. Cleaner Prod.*, **171**, 1605-1621. https://doi.org/10.1016/j.jclepro.2017.10.102.

Morsy, M.S., Abbas, H. and Alsayed, S.H. (2012), "Behavior of blended cement mortars containing nano-metakaolin at elevated temperatures", *Construct. Build. Mater.*, **35**, 900-905. https://doi.org/10.1016/j.conbuildmat.2012.04.099.

Murray, C.A., Snyder, K.S. and Marion, B.A. (2014), "Characterization of permeable pavement materials based on recycled rubber and chitosan", *Construct. Build. Mater.*, **69**, 221-231. https://doi.org/10.1016/j.conbuildmat.2014.07.047.

Nambiar, E.K. and Ramamurthy, K. (2006), "Models relating mixture composition to the density and strength of foam concrete using response surface methodology", *Cement Concrete Compos.*, **28**, 752-760. https://doi.org/10.1016/j.cemconcomp.2006.06.001.

Nassar, A.I., Thom, N. and Parry, T. (2016), "Optimizing the mix design of cold bitumen emulsion mixtures using response surface methodology", *Construct. Build. Mater.*, **104**, 216-229.

https://doi.org/10.1016/j.conbuildmat.2015.12.073.
Nikbin, I.M., Davoodi, M.R., Fallahnejad, H. and Rahimi, S. (2016), "Influence of mineral powder content on the fracture behaviors and ductility of self-compacting concrete", *J. Mater. Civ. Eng.*, **28**(3). https://doi.org/10.1061/(ASCE)MT.1943-5533.0001404.
Rezaifar, O., Hasanzadeh, M. and Gholhaki, M. (2016), "Concrete made with hybrid blends of crumb rubber and metakaolin: Optimization using Response Surface Method", *Construct. Build. Mater.*, **123**, 59-68. https://doi.org/10.1016/j.conbuildmat.2016.06.047.
Ritter, A. and Muñoz-Carpena, R. (2013), "Performance evaluation of hydrological models: statistical significance for reducing subjectivity in goodness-of-fit assessments", *J. Hydrol.*, **480**, 33-45. https://doi.org/10.1016/j.jhydrol.2012.12.004.
Rostamiyan, Y., Fereidoon, A., Mashhadzadeh, A.H., RezaeiAshtiyani, M. and Salmankhani, A. (2015), "Using response surface methodology for modeling and optimizing tensile and impact strength properties of fiber orientated quaternary hybrid nano composite", *Compos: Part B.*, **69**, 304-316. https://doi.org/10.1016/j.compositesb.2014.09.031.
Sahmaran, M. and Li, V.C. (2007), "De-icing salt scaling resistance of mechanically loaded engineered cementitious composites", *Cement Concrete Res.*, **37**, 1035-1046. https://doi.org/10.1016/j.cemconres.2007.04.001.
Şahmaran, M., Lachemi, M. and Li, V.C. (2010), "Assessing Mechanical Properties and Microstructure of Fire-Damaged Engineered Cementitious Composites", *ACI Mater.*, **107**(3), 297-304. https://doi.org/10.14359/51663759.
Şahmaran, M., Özbay, E., Yücel, H.E., Lachemi, M. and Li, V.C. (2011), "Effect of fly ash and PVA fiber on microstructural damage and residual properties of engineered cementitious composites exposed to high temperatures", *J. Mater. Civ. Eng.*, **23**, 1735-1745. https://doi/10.1061/%28ASCE%29MT.1943-5533.0000335 .
Salehi, H. and Mazloom, M. (2018), "Effect of magnetic-field intensity on fracture behaviors of self-compacting lightweight concrete", *Mag. Concrete Res.*, **71**(13), 665-679. https://doi.org/10.1680/jmacr.17.00418.
Salehi, H. and Mazloom, M. (2019a), "Opposite effects of ground granulated blast-furnace slag and silica fume on the fracture behavior of self-compacting lightweight concrete", *Construct. Build. Mater.*, **222**, 622-632. https://doi.org/10.1016/j.conbuildmat.2019.06.183.
Salehi, H. and Mazloom, M. (2019b), "An experimental investigation on fracture parameters and brittleness of self-compacting lightweight concrete containing magnetic field treated water", *Arch. Civil Mech. Eng.*, **19**, 803-819. https://doi.org/10.1016/j.acme.2018.10.008.
Sandeep, M.S., Nagarajan, P., Shashikala, A.P. and Habeeb, S.A. (2016), "Determination of strut efficiency factor for concrete deep beams with and without fiber", *Advan. Comput. Des.*, **1**(3), 253-264. http://dx.doi.org/10.12989/acd.2016.1.3.253.
Şimşek, B., Uygunoğlub, T., Korucua, H.M. and Kocakerim, M.M. (2018), "Analysis of the effects of dioctyl terephthalate obtained from polyethylene terephthalate wastes on concrete mortar: A response surface methodology-based desirability function approach application", *J. Cleaner Prod.*, **170**, 437-445. https://doi.org/10.1016/j.jclepro.2017.09.176.
Tyagi, M., Rana, A., Kumari, S. and Jagadevan, S. (2018), "Adsorptive removal of cyanide from coke oven wastewater onto zero-valent iron: Optimization through response surface methodology, isotherm and kinetic studies", *J. Cleaner Prod.*, **178**, 398-407.
Varughese, J.A. and Nikithan, S. (2016), "Seismic behavior of concrete gravity dams", *Advan. Comput. Des.*, **1**(2), 195-206. http://dx.doi.org/10.12989/acd.2016.1.2.195.
Yang, E. and Li, V.C. (2010), "Strain-hardening fiber cement optimization and component tailoring by means of a micromechanical model", *Constr. Build. Mater.*, **24**, 130-139. https://doi.org/10.1016/j.conbuildmat.2007.05.014.
Yang, E.H., Sahmaran, M., Yang, Y. and Li, V.C. (2009), "Rheo- logical control in production of engineered cementitious composites", *ACI Mater.*, **106**(4), 357-366.

Yu, J., Lin, J., Zhang, Z. and Li, V.C. (2015), "Mechanical performance of ECC with high-volume fly ash after sub-elevated temperatures", *Construct. Build. Mater.*, **99**, 82-89. https://doi.org/10.1016/j.conbuildmat.2015.09.002.

Yu, J., Weng, W. and Yu, K. (2014), "Effect of different cooling regimes on the mechanical properties of cementitious composites subjected to high temperatures", https://doi.org/10.1155/2014/289213.

Zhang, J., Wang, Z., Ju, X. and Shi, Z. (2014), "Simulation of flexural performance of layered ECC-concrete composite beam with fracture mechanics model", *Eng. Fract. Mech.*, https://doi.org/10.1016/j.engfracmech.2014.08.016.

Zhang, Y., Liu, Z. and Yao, L. (2019), "Mechanical properties of high-ductility cementitious composites with methyl silicone oil", *Mag. Concrete Res.*, 1-10. https://doi.org/10.1680/jmacr.18.00192.

Zhu, Z. and Gu, D. (2016), "Formulation design of chloride-free cement additive by response surface methodology", *Advan. Comput. Des.*, **1**(1), 27-35. http://dx.doi.org/10.12989/acd.2016.1.1.027.

TK